Thermochimica Acta 494 (2009) 110–114

Contents lists available at ScienceDirect

Thermochimica Acta

journal homepage: www.elsevier.com/locate/tca

Crystallisation kinetics of a cesium iron phosphate glass

Kitheri Joseph, R. Venkata Krishnan, K.V. Govindan Kutty, P.R. Vasudeva Rao*

Chemistry Group, Indira Gandhi Centre for Atomic Research, Kalpakkam, Tamil Nadu, India

ARTICLE INFO

Article history:
Received 4 February 2009
Received in revised form 28 April 2009
Accepted 30 April 2009
Available online 15 May 2009

Keywords:
Cesium iron phosphate glass
Differential scanning calorimetry
Non-isothermal
Crystallisation kinetics
Isoconversional method
Activation energy

ABSTRACT

The crystallisation kinetics of 36 mol% Cs_2O–26 mol% Fe_2O_3–P_2O_5 glass was studied by differential scanning calorimetry under non-isothermal conditions at various heating rates. X-ray diffraction technique was employed to understand the product of crystallisation. This glass crystallises to a mixture of $CsFe(P_2O_7)$, $Cs_7Fe_7(PO_4)_8O_2$ and Cs_3PO_4. The activation energy of the crystallisation process was determined by classical multi heating rate methods like Kissinger, Mahadevan and Augis–Bennet. Heating rate dependence of the activation energy was observed when the data were analysed using Coats and Redfern method. This dependence of the activation energy was evaluated by the application of Kissinger–Akahira–Sunrose isoconversional method. It was observed that the activation energy of crystallisation was found to vary with the degree of conversion. The value of Avrami exponent '*n*' obtained was 4, suggesting the mechanism of crystallisation to be bulk nucleation and three-dimensional growth.

© 2009 Elsevier B.V. All rights reserved.

1. Introduction

Radioactive ^{137}Cs extracted from the high level nuclear waste can be immobilised in a suitable vitreous matrix and used as radioactive source for medical purposes [1]. Iron phosphate glass is one such potential vitreous matrix for cesium [2]. In our previous studies, it was demonstrated that up to 36 mol% Cs_2O (inactive) could be immobilised in iron phosphate matrix without crystallisation or phase separation [3]. This glass is referred as IP5C5 throughout this paper. Thermal stability of IP5C5 glass needs to be explored in order to understand the crystallisation/devitrification behaviour of the system. Differential scanning calorimetry (DSC) is a suitable technique to study the crystallisation process [4–6] of glasses under isothermal or non-isothermal conditions. By knowing the temperature of crystallisation and fraction of crystallisation (degree of conversion), the kinetic parameter E_c (activation energy of crystallisation), can be obtained. The objectives of the present work are to determine the activation energy of crystallisation and to identify the phases formed after crystallisation. DSC was employed under non-isothermal condition to derive the activation energy of crystallisation and to understand the mechanism of crystallisation of the IP5C5 glass, and X-ray diffraction (XRD) technique to characterise the crystallised products. The activation energy of crystallisation was determined by using two different methods: classic and isoconversion.

2. Experimental

Cs_2CO_3 (99.9%, Aldrich), Fe_2O_3 (99.5%, Fisher Scientific), $NH_4H_2PO_4$ (ADP) (99%, Ranbaxy) were mixed in appropriate amounts and calcined at 873 K and melted in a Pt crucible at 1263 K in air for 1 h to get cesium loaded iron phosphate glass of the composition 36 mol% Cs_2O–26 mol% Fe_2O_3–P_2O_5 [3]. The melt was air-quenched. The quenched sample was ball milled and the amorphous state of the sample was checked by XRD technique (Siemens D500 X-ray diffractometer employing Cu Kα radiation).

Crystallisation kinetics of the glass powder was studied by employing DSC (M/s. Mettler Toledo model DSC 821e/700) under flowing argon at a flow of 50 ml/min. DSC was calibrated for temperature as explained in Ref. [7] and the accuracy of temperature measurement was ±1 K. Nearly 7 mg of sample was taken in the Pt crucible and experiments were carried out at the heating rates of 5, 7, 10 and 15 K/min. The variations in the quantity of the sample used in the DSC measurements were within ±2 μg.

The glass powders were annealed separately at 858 K in the Pt crucible in flowing argon to identify the crystallisation products by XRD technique. The weight of the sample was measured before and after annealing. There was no observable weight change after annealing, confirming that there was no loss of material during annealing.

3. Results and discussion

The amorphous state of the IP5C5 glass was confirmed by XRD as shown in Fig. 1.

* Corresponding author. Fax: +91 44 2748 0065.
E-mail address: vasu@igcar.gov.in (P.R. Vasudeva Rao).

0040-6031/$ – see front matter © 2009 Elsevier B.V. All rights reserved.
doi:10.1016/j.tca.2009.04.027

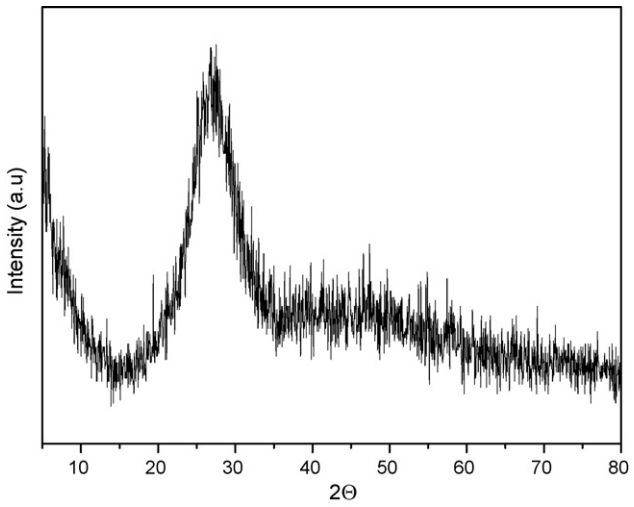

Fig. 1. XRD pattern of the IP5C5 glass.

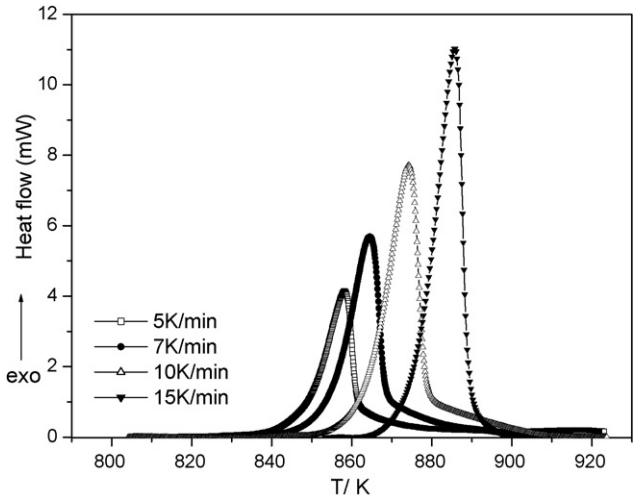

Fig. 3. DSC curves of IP5C5 glass (Ar atmosphere; flow rate: 50 ml/min).

3.1. Characterisation of the crystallised products

The XRD pattern of the product of crystallisation is shown in Fig. 2. The constitution of the crystalline phases formed by annealing the glass was determined by knowing the chemical composition [3] and by the XRD technique. The XRD pattern of the crystallised product indicated the presence of $CsFeP_2O_7$ and $Cs_7Fe_7(PO_4)_8O_2$. A mixture of these two phases alone is not sufficient to account for the composition of the glass. The unaccounted portion conforms to Cs_3PO_4. The XRD lines corresponding to Cs_3PO_4 (JCPDS 26-1097) coincide with some of the less intense peaks of $CsFeP_2O_7$ and $Cs_7Fe_7(PO_4)_8O_2$. By assigning these less intense peaks to Cs_3PO_4, the crystallised product could be matched with the overall chemical composition of the glass. Thus, the IP5C5 glass crystallises to a mixture of $CsFeP_2O_7$ (JCPDS 81-2403), $Cs_7Fe_7(PO_4)_8O_2$ (JCPDS 84-1611) and Cs_3PO_4 (JCPDS 26-1097).

3.2. Kinetic analysis

DSC curves of the IP5C5 glass at various heating rates in the temperature range of 805–920 K are presented in Fig. 3. As expected [8–11], the onset temperatures of crystallisation were found to have linear dependency with heating rate as shown in Fig. 4a. The actual crystallisation temperature was obtained by extrapolating the linear fit to zero heating rate and was found to be 818 K.

From the DSC data, the activation energy of crystallisation (E_c) was evaluated by classical methods and isoconversional methods as described in the following sections.

The rate of any heterogeneous reaction under non-isothermal condition can be expressed as [12],

$$\frac{d\alpha}{dT} = \frac{k(T)}{\beta} f(\alpha) \tag{1}$$

where α is the fraction of crystallisation or degree of conversion at temperature T (absolute temperature), $f(\alpha)$ the conversion function which is dependent on the mechanism of the reaction, β the rate of heating, and $k(T)$ is the temperature dependent rate constant. The integral form of the Eq. (1) can be represented as:

$$g(\alpha) \equiv \int_0^{\alpha} \frac{d(\alpha)}{f(\alpha)} = \int_0^{T} \left(\frac{A}{\beta}\right) \exp\left[\frac{-E_c}{RT}\right] dT \tag{2}$$

where $g(\alpha)$ is the integral form of $f(\alpha)$, A the pre-exponential factor, E_c the activation energy of reaction and R is the gas constant.

Among the various methods of estimation of crystallisation kinetics under linear heating rate, the following classical methods were employed to determine the activation energy of crystallisation.

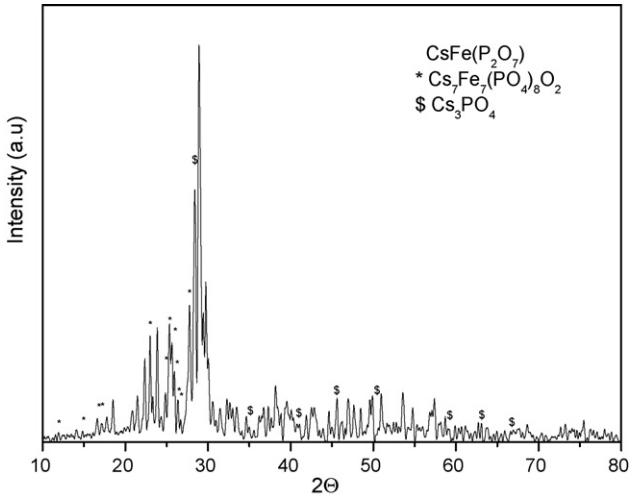

Fig. 2. XRD pattern of the crystallised products of IP5C5 at 858 K.

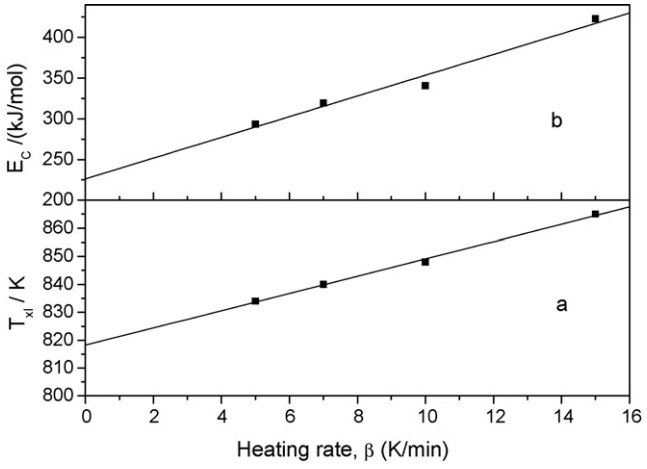

Fig. 4. (a) Crystallisation temperature (T_{xl}) as a function of heating rate, the fitted line is also shown. (b) Effective activation energy as a function of heating rate; solid line shows the linear fit.

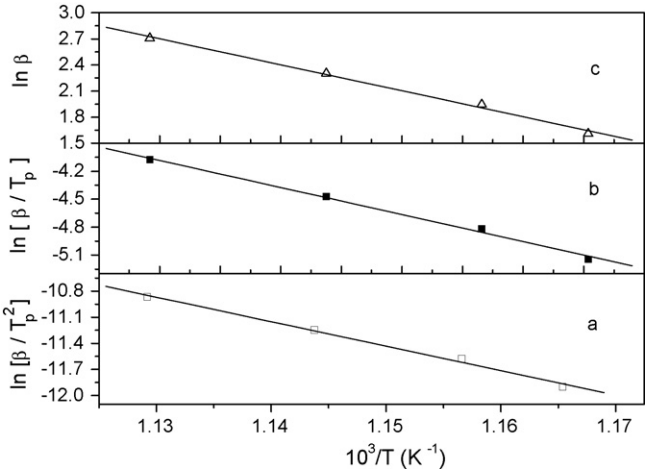

Fig. 5. Physical model independent methods: (a) Kissinger method; (b) Augis–Bennet method; (c) Mahadevan method.

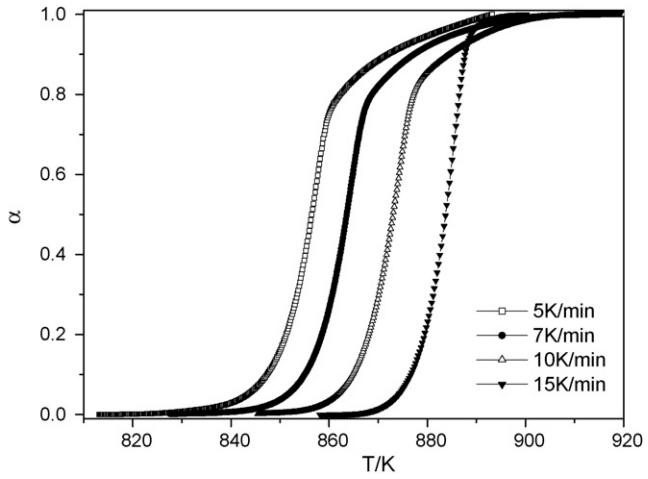

Fig. 6. Fraction of crystallisation (α) as a function of temperature at various heating rates.

3.2.1. Kissinger method

The activation energy of crystallisation can be obtained by applying the Kissinger method of kinetic analysis [13].

$$\ln\frac{\beta}{T_p^2} = -\frac{E_c}{RT_p} + \text{const} \quad (3)$$

The slope of the plot of $\ln(b/T_p^2)$ vs. $1/T_p$ gives the value of E_c. The Kissinger plot is shown in Fig. 5a. The value of activation energy obtained by the Kissinger method is 234 ± 12 kJ/mol.

3.2.2. Augis and Bennet method

The activation energy of crystallisation was also determined by applying the reduced Augis–Bennet method [14],

$$\ln\frac{\beta}{T_p} = -\frac{E_c}{RT_p} + \ln k_0 \quad (4)$$

where k_0 is a constant. According to this method, a plot of $\ln(\beta/T_p)$ vs. $1/T_p$ gives a linear fit, where T_p is the peak temperature of crystallisation at various heating rates. The activation energy is evaluated from the slope of the linear plot and the value is found to be 241 ± 12 kJ/mol. The plot of $\ln(\beta/T_p)$ vs. $1/T_p$ is shown in Fig. 5b.

3.2.3. Method of Mahadevan et al.

According to Mahadevan et al. [15], the relation between $\ln\beta$ and the activation energy of crystallisation can be expressed as:

$$\ln\beta = -\frac{E_c}{RT_p} + \text{const} \quad (5)$$

The activation energy of crystallisation was obtained by plotting $\ln\beta$ vs. $1/T_p$ (Fig. 5c). The value of E_c was deduced to be 248 ± 12 kJ/mol and it is in agreement with those obtained by using the other model free methods.

3.2.4. Isoconversional methods

From the DSC curve, α (the fraction of crystallisation) was determined in the usual way [16] as a function of temperature at various heating rates. The plot of α as a function of temperature is shown in Fig. 6. The Kissinger–Akahir–Sunose (KAS) [17,18] isoconversional method employs the following equation to evaluate the activation energy of crystallisation as a function of α,

$$\ln\frac{\beta_i}{T_{\alpha,i}^2} = \text{const} - \frac{E_\alpha}{RT_{\alpha,i}} \quad (6)$$

where the subscript 'i' denotes the various heating rates. The slope of the plot $\ln(b_i/T_{\alpha,i}^2)$ vs. $1/T_{\alpha,i}$ gives the value of effective activation energy E_α. The plot of E_α as function of α is shown in Fig. 7. From this figure, it is clear that the effective activation energy increases as a function of α up to the value of 0.1. For the α value of 0.1–0.75, only a small increase is observed, and the average value (232 ± 16 kJ/mol) within this α range matches with the value obtained by using the previous methods. The effective activation energy is found to increase beyond the α value of 0.75.

3.3. Study of crystallisation mechanism

The following Coats and Redfern equation [19] was employed to determine the mechanism of crystallisation:

$$\ln\left[\frac{g(\alpha)}{T^2}\right] = \ln\left[\frac{AR}{\beta E_c}\left(1 - \frac{2RT}{E_c}\right)\right] - \frac{E_c}{RT} \quad (7)$$

The various expressions of $g(\alpha)$ functions that are tested in this work are taken from Ref. [20]. A plot of $\ln(g(\alpha)/T^2)$ vs. $1/T$ gives a straight line when an appropriate $g(\alpha)$ function is used in this equation. The mechanism of the reaction is given by the $g(\alpha)$ function. The possible mechanism was chosen based on the best linear fit with highest correlation co-efficient and low standard deviation. The best fit was obtained for the Avrami–Erofeev nucleation and growth model (A4) with 'n' (Avrami-exponent) as 4 in the α range of 0.1–0.75. The plot of $\ln(g(\alpha)/T^2)$ vs. $1/T$ as a function of the heating rate is shown in Fig. 8, where the $g(\alpha) = [-\ln(1-\alpha)]^{1/4}$. Generally the value of the Avrami exponent 'n' is equal to m or $m+1$, where m

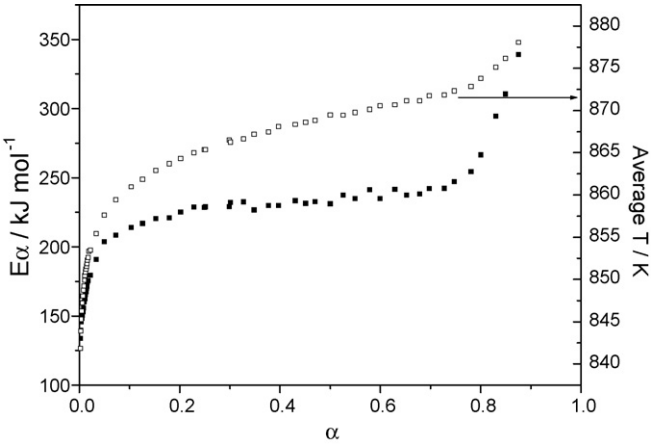

Fig. 7. Plot of E_α and average temperature T (K) as a function of α.

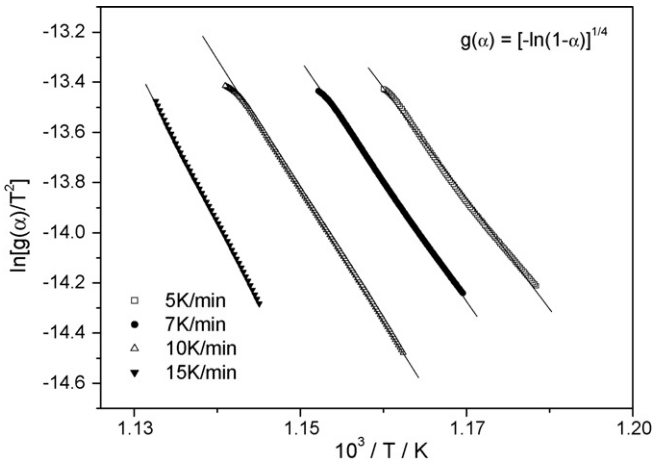

Fig. 8. Plot of $\ln(g(\alpha)/T^2)$ vs. $1/T$ at various β, where $g(\alpha) = (-\ln(1-\alpha))^{1/4}$; the fitted line is also shown.

denotes the dimension of the growth of the nuclei of crystallisation [21–23]. When the nuclei are formed during the heat treatment prior to the thermal analysis, the value of n equals that of m. When the nuclei are formed during the heating run at constant β, the n is equal to $m+1$. For the present crystallisation studies, the nuclei were formed during heating in the DSC. Hence, $n = m+1$ for our experiments. The value of m corresponds to 3, which indicates that the growth of nuclei occurs in all three dimensions [22,23].

The Avrami exponent 'n' can be confirmed by the method described below. The fraction of crystallisation (α) at the constant heating rate (β) is related to the activation energy of crystallisation by the equation [24],

$$\frac{d\ln[-\ln(1-\alpha)]}{d(1/T)} \cong -\frac{nE_c}{R} \quad (8)$$

The value of n depends on the dimensionality of crystal growth. The plot of $\ln[-\ln(1-\alpha)]$ vs. $1/T$ gives linear fit for a fixed β, which is shown in Fig. 9. From the slope, the values of nE_c can be obtained. Using the value of E_c evaluated from the Coats and Redfern method under various β, the value of n is evaluated and listed in Table 1. The value of n is in good agreement with the expected value of 4 (obtained by physical model dependent method), indicating that the crystallisation mechanism involves nucleation and three-dimensional growth.

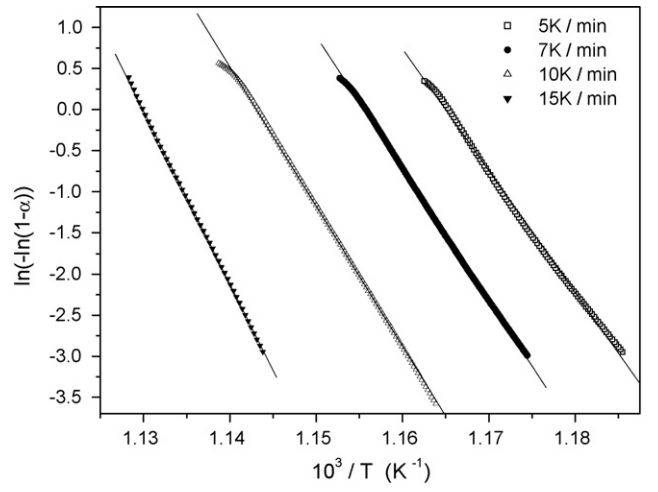

Fig. 9. Plot of $\ln(-\ln(1-\alpha))$ vs. $1/T$ at various heating rates; solid line shows the linear fit.

Table 1
Evaluation of Avrami exponent 'n'.

Heating rate, β (K/min)	nE_c	E_c [a] (kJ/mol)	n
5	1230	293	4.20
7	1335	319	4.18
10	1414	340	4.16
15	1751	423	4.14

[a] From Coats and Redfern method.

Theoretically, the activation energy of crystallisation can also be obtained from Coats and Redfern physical model dependent method. For the IP5C5 glass, the activation energy found to increase with heating rate. The effective activation energy was obtained by plotting the dependence of the activation energy on β and extrapolating it to $\beta = 0$. The effective activation energy would correspond to 226 ± 14 kJ/mol at $\beta = 0$ in the plot of its dependence on β (Fig. 4b). Basically, in this model-fitting method, the activation energy is assumed to be constant. Then the E_c is not expected to change with the heating rate. However, our results show that the activation energy obtained by physical model dependent method increase with β. Thus the assumption of constant activation energy is not appropriate in the model-fitting method. This shows the drawback of the physical model dependent method. Hence it is preferable to use isoconversional and multi heating rate methods [25] for the evaluation of activation energy.

In order to understand the increase in activation energy as a function of heating rate, the temperature dependence of the effective activation energy was also evaluated by replacing α with an average T [26] using the plots of α vs. T (Fig. 5). The increase in average temperature as a function of α (Fig. 8) indicates the occurrence of concurrent (competitive) reactions [27] during crystallisation. In the present crystallisation process, the glass crystallises simultaneously into three different phases, and this could be the reason for the increase in activation energy as a function of temperature and conversion. Though the effective activation energy of crystallisation of this glass obtained by physical model dependent method matches (within the experimental uncertainty) with that from isoconversional method in the α range of 0.1–0.75, isoconversional method are more popular and recommended [28] because of their ability to determine the activation energy as a function of degree of conversion and temperature.

4. Conclusion

The crystallisation kinetics of 36 mol% Cs_2O–26 mol% Fe_2O_3–P_2O_5 glass was studied by DSC under non-isothermal conditions. The glass and the crystallised products were characterised by XRD. The glass was found to crystallise into a mixture of $CsFe(P_2O_7)$, $Cs_7Fe_7(PO_4)_8O_2$ and Cs_3PO_4. The activation energy of crystallisation was evaluated by Kissinger, Mahadevan, Augis–Bennet and isoconversional methods. Simultaneous crystallisation of the glass into three different phases could be the reason for the increase in activation energy as a function of the temperature and conversion. The obtained Avrami parameter ($n = 4$), reveals the crystallisation mechanism to be controlled by bulk nucleation with three-dimensional growth.

Acknowledgements

The authors thank Shri. R. Asuvathraman for his kind help during the calculation of kinetic parameters. The authors thank Dr. K. Ananthasivan for his fruitful suggestions. The authors also thank Dr. K. Nagarajan for his support during DSC runs. The authors also thank Professor Sergey Vyazovkin, Professor at University of Alabama at Birmingham for providing valuable suggestions in improving this manuscript.

References

[1] Sharing Innovative Experiences, Fighting Cancer with Cesium: India, Examples of successful initiatives in science and technology in the South, vol. 1, Published in partnership with Third World Academy of Sciences (TWAS) and Third World Network of Scientific Organisation (TWNSO), 1999, pp. 138–145.
[2] M.G. Mesko, D.E. Day, B.C. Bunker, Waste Manage. 20 (2000) 271–278.
[3] K. Joseph, K.V. Govindan Kutty, P. Chandramohan, P.R. Vasudeva Rao, J. Nucl. Mater. 384 (2009) 262–267.
[4] I.W. Donald, J. Non-Cryst. Solids 345/346 (2004) 120–126.
[5] N. Afify, J. Non-Cryst. Solids 142 (1992) 247–259.
[6] J. Colmenero, J.M. Barandiaran, J. Non-Cryst. Solids 30 (1979) 263–271.
[7] R. Venkata Krishnan, K. Nagarajan, Thermochim. Acta 440 (2006) 141–145.
[8] A.F. Kozmidis-Petrovic, G.R. Strbac, D.D. Strbac, J. Non-Cryst. Solids 353 (2007) 2014–2019.
[9] J. Vazquez, D. Garcia, G. Barreda, P.L. Lopez-Alemany, P. Villares, R. Jimenez-Garay, J. Non-Cryst. Solids 345/346 (2004) 142–147.
[10] V.C.S. Reynoso, K. Yukimitu, T. Nagami, C.L. Carvalho, J.C.S. Moraes, E.B. Araujo, J. Phys. Chem. Solids 64 (2003) 27–30.
[11] B.J. Costa, M. Poulain, Y. Messaddeq, S.J.L. Ribeiro, J. Non-Cryst. Solids 273 (2000) 76–80.
[12] M.E. Brown, D. Dollimore, A.K. Galwey, Comprehensive Chemical kinetics, vol. 22, Elsevier, Amsterdam, 1988, p. 99.
[13] H.E. Kissinger, Anal. Chem. 29 (1957) 1702–1706.
[14] J.A. Augis, J.E. Bennett, J. Thermal Anal. 13 (1978) 283–292.
[15] S. Mahadevan, A. Giridhar, A.K. Singh, J. Non-Cryst. Solids 88 (1986) 11–34.
[16] A. Catalani, M.G. Bonicelli, Thermochim. Acta 438 (2005) 126–129.
[17] A.A. Abu-Sehly, Thermochim. Acta 485 (2009) 14–19.
[18] A.A. Joraid, Thermochim. Acta 456 (2007) 1–6.
[19] A.N. Coats, J.P. Redfern, Nature 201 (1964) 68–69.
[20] S. Vyazovkin, J. Thermal Anal. Calor. 83 (2006) 45–51.
[21] K. Matusita, T. Konatsu, R. Yorota, J. Mater. Sci 19 (1984) 291–296.
[22] K. Matusita, S. Sakka, J. Non-Cryst. Solids 38/39 (1980) 741–746.
[23] H.A. Hashem, Abouelhassen, Fizika (A) 15 (2006) 237–250.
[24] J. Malek, Thermochim. Acta 355 (2000) 239–253.
[25] M.E. Brown, et al., Thermochim. Acta 355 (2000) 125–143.
[26] S. Vyazovkin, I. Dranca, Macromol. Chem. Phys. 207 (2006) 20–25.
[27] S. Vyazovkin, A.I. Lesnikovich, Thermochim. Acta 165 (1990) 273–280.
[28] S. Vyazovkin, C.A. Wight, Thermochim. Acta 340/341 (1999) 53–68.